

Loughborough University  
Institutional Repository

---

*Effects of closed immersion  
filtered water flow velocity  
on the ablation threshold of  
bisphenol A polycarbonate  
during excimer laser  
machining.*

This item was submitted to Loughborough University's Institutional Repository by the/an author.

**Citation:** DOWDING, C.F., LAWRENCE, J. and HOLMES, A., 2010. Effects of closed immersion filtered water flow velocity on the ablation threshold of bisphenol A polycarbonate during excimer laser machining. *Applied Surface Science*, 256(12), pp.3705-3713

**Additional Information:**

- This article was published in the journal *Applied Surface Science* [© Elsevier] and is available at: <http://dx.doi.org/10.1016/j.apsusc.2010.01.009>

**Metadata Record:** <https://dspace.lboro.ac.uk/2134/6397>

**Version:** Accepted for publication

**Publisher:** © Elsevier

Please cite the published version.

This item was submitted to Loughborough's Institutional Repository (<https://dspace.lboro.ac.uk/>) by the author and is made available under the following Creative Commons Licence conditions.



For the full text of this licence, please go to:  
<http://creativecommons.org/licenses/by-nc-nd/2.5/>

Effects of closed immersion filtered water flow velocity on the ablation threshold of  
bisphenol A polycarbonate during excimer laser machining.

Colin Dowding \*

Jonathan Lawrence \*

Andrew Holmes †

\* Wolfson School of Mechanical and Manufacturing Engineering, Loughborough  
University, Loughborough, Leicestershire. LE11 3TU. United Kingdom.

† Department of Electrical and Electronic Engineering, Imperial College London, South  
Kensington Campus, SW2 2AZ, United Kingdom.

Correspondence

Mr. Colin Dowding

Wolfson School of Mechanical and Manufacturing Engineering,

Loughborough University,

Leicestershire,

LE11 3TU,

Great Britain.

Tel : +44 (0)1509 227593

Fax : +44 (0)1509 227648

e-mail : [c.f.dowding@lboro.ac.uk](mailto:c.f.dowding@lboro.ac.uk)

### Abstract:

A closed flowing thick film filtered water immersion technique ensures a controlled geometry for both the optical interfaces of the flowing liquid film and allows repeatable control of flow-rate during machining. This has the action of preventing splashing, ensures repeatable machining conditions and allows control of liquid flow velocity. To investigate the impact of this technique on ablation threshold, bisphenol A polycarbonate samples have been machined using KrF excimer laser radiation passing through a medium of filtered water flowing at a number of flow velocities, that are controllable by modifying the liquid flow rates. An average decrease in ablation threshold of 7.5% when using turbulent flow velocity regime closed thick film filtered water immersed ablation, compared to ablation using a similar beam in ambient air; however, the use of laminar flow velocities resulted in negligible differences between closed flowing thick film filtered water immersion and ambient air. Plotting the recorded threshold fluence achieved with varying flow velocity showed that an optimum flow velocity of 3.00 m/s existed which yielded a minimum ablation threshold of 112 mJ/cm<sup>2</sup>. This is attributed to the distortion of the ablation plume effected by the flowing immersion fluid changing the ablation mechanism: at laminar flow velocities *Bremsstrahlung* attenuation decreases etch rate, at excessive flow velocities the plume is completely destroyed, removing the effect of plume etching. Laminar flow velocity regime ablation is limited by slow removal of debris causing a non-linear etch rate over 'n' pulses which is a result of debris produced by one pulse remaining suspended over the feature for the next pulse. The impact of closed thick film filtered water immersed ablation is dependant upon beam fluence: high fluence beams achieved greater etch efficiency at high flow velocities as the effect of *Bremsstrahlung* attenuation is removed by the action of the fluid on the plume; low fluences loose efficiency as the beam makes proportionally large fluence losses at it passes through the chamber window and immersion medium.

## Introduction

Laser ablation is at the vanguard of the micro and nano manufacturing industries [1-3]. This technology has been continuously refined and improved upon in terms of laser fluence, optical resolution and production speed since the emergence of the technique in the late 1970s [3]. However, one area has continued to plague the laser ablation pattern machining sector: laser ablation generated debris [4]. Debris can contribute to beam attenuation after ejection but before deposition [5]. Debris can be generated in a mode that coats unimportant areas, areas still to be machined or worse still, features that have already been machined [6]. Thus, debris poses a direct threat of lowering manufacturing yield by these means. To compound matters, debris can coat machinery, requiring costly downtime for cleaning and servicing [7], or the debris can become airborne in the working environment of tool users, posing potential respiratory health issues [8]. The use a technique involving closed flowing thick film filtered water immersion of the sample during laser ablation has shown promise as a plausible solution for such problems [9, 10]; however, the impact of such techniques on the basic laser machining characteristics are not extensively documented; only the effect of thin film open immersion on ablation rate and threshold having been previously detailed [11, 12]. This work will explore the impact of closed flowing thick film filtered water immersion laser ablation machining using KrF excimer laser radiation on the ablation threshold of bisphenol A polycarbonate in comparison to the machining properties of the same material in ambient air and, furthermore, the importance of liquid flow velocity,  $V$ , to the ablation threshold will also be explored in detail in this work.

The threshold fluence of laser ablation is useful in assessing the efficiency of a laser machining system at material removal. Losses in equipment or media surrounding the substrate will be most evidently be evidenced by use of this measureand, as it describes the minimum energy required from the laser for material ablation to commence []. The threshold

is measured as a Beers law relationship, and thus a predicted threshold value (where surface modification ends and ablation commences) can be interpolated [].

In gaseous or vacuum media, various mechanisms such as phase explosion and surface evaporation [15, 16], photothermal effects [17, 18] or photomechanical and acoustic interactions [19] act individually or in a combination thereof, as discussed in the review of Georgiou and Koubenakis [20]; moreover, Prasad *et al.* have conducted extensive effort into modelling such interactions [21]. The introduction of a liquid to this system poses a significant modification to the interaction typical in gaseous or vacuum environments normally used for machining [22, 23, 24-27]. A technique for delivering a long wavelength laser wavelength by use of a fine jet of water proves that use of such mediums do not pose unacceptable attenuation of the beam [28]. When using liquid as a media for laser ablation, Zhu *et al.* [23] demonstrated that a threshold film thickness for immersing liquids exists, lying at 1.1 mm. using a closed flowing thick film filtered water immersion depth below this value significantly reduces the ablation rate compared to that of ablation in ambient air. Use of an immersing liquid depth greater than the 1.1 mm value and the opposite is true. The cause of this is identified and explained by Dowding and Lawrence [11], where splashing is witnessed when using thin film regime flowing open immersion – thus signifying the explosive rupture of the immersing thin film of liquid by the ablation plume, which negated all action of ablation plume etching. Simultaneously, the immersing liquid film contained the plume long enough to significantly reduce laser etching by *Bremstrahlung* attenuation. This theory relies on the principle of acoustic type surface etching as described by Dyer *et al.* [29], where violent excitation of the substrate surface layers results in shear cracking and then ejection of solid species from the surface; application of a confined ablation plume, as can be produced by closed flowing thick film filtered water immersion will amplify such acoustic effects. Also, the ejection of surface melt and advent of surface evaporation, generated by

ablation plume heating, a probable phenomenon in gaseous media [14], will be amplified by the action of thermodynamic compression of the ablation plume by the confining liquid media. The existence and efficacy of ablation plume etching can be proven by the example of laser induced backside wet etching (LIBWE), pioneered by Wang *et al.* [30] LIBWE has been shown to reduce laser ablation threshold fluence for wavelength transparent materials, such as Quartz for excimer laser applications, by more than an order of magnitude [31, 32]. Work has been conducted to investigate the effect of open immersion on the ablation rate of excimer laser ablation of bisphenol a polycarbonate [27, 11, 12,]. A number of limitations were observed and causes diagnosed. Splashing was a common occurrence during machining. This was attributed to irregular but broadly increased plume pressure, which significantly attenuates the laser beam *en-route* to the sample surface [12]. In a thick film regime, the volume of liquid above the ablation plume confines the plume expansion and prevents it from free expansion in the manner allowed by the less viscous medium of ambient air, thus the compressed, high pressure ablation plume attacks the surface of the sample to be machined causing a high etch rate due to the plume which more than compensates for the loss of laser etching due to inverse *Bremstrahlung* attenuation [23, 24, 25, 12]. When using open thin film immersion, the same volume of liquid is not available to confine the ablation plume pressure, causing a threshold pressure exists in this condition; once exceeded, rupture occurs and plume gas escapes violently from the covering liquid film into the ambient air above, producing liquid splashing as a by-product [12]. The action of turbulence, instigated by the non-symmetrical drag profile, combined with the strong contribution of meniscus instability such as inertial, capillary and viscous effects, described schematically in Figure 1(a), of a flow running across a flat plate in the open flow immersion technique allowed surface ripple to occur and thence the depth of liquid above the plume varied with respect to time and position above the sample, this results in an irregular and non-repeatable plume etch-rate.

This is witnessed by the fluctuation between ablation depths with increasing numbers of laser pulses that should have produced a linear relationship in a regular, repeatable surrounding medium.

The use of a closed ablation chamber has removed the variance of the flow geometry both with respect to time and position above the sample to be machined by ensuring the drag on the boundaries of the flow symmetrical about the centre of the flow, as described schematically in Figure 1(b), and removes the meniscus that dominates flow characteristics in open flows. These two factors combined result in reduced eddy generation. A drawback of having a sealed flow is that thin film regimes (less than 1.1mm in thickness [23]) could allow the compressed ablation plume to extend through the flowing liquid from the sample surface to the bottom surface of the chamber window, potentially plume etching the window and permanently damaging a critical component in the optical path of the beam. Hence, the experiments conducted in this work are of the thick film regime to prolong the life of the chamber window. Nevertheless, the use of a closed flow chamber guarantees optical geometry of the final medium before the sample and maintains a repeatable and regular containment of the ablation plume during and after laser pulses. Because of this, the closed flow geometry equipment allows the authors to directly investigate the importance and action of liquid flow velocity, a parameter that is controllable by modifying the flow rate,  $Q$ , on the fundamental ablation characteristics of closed flowing thick film filtered water immersion.

## Experimental Procedures

### Material Details

Bisphenol A polycarbonate (Holbourne Plastics, Ltd), was as received in 1200 x 1000 mm<sup>2</sup> sheets of 0.5 mm thickness. Prior to excimer laser processing, the bisphenol A polycarbonate sheet was cut into rectangular sections of 8 x 12 mm<sup>2</sup> using scissors - a shear cutting

technique which avoids production of debris. Protective cover sheets were then peeled off each sample.

### Laser Details and Experimental Set-Up.

For both closed flowing thick film filtered water immersion and ambient air processing, an excimer laser (LPX200; Lambda Physique, GmbH) using KrF as the excitation medium was used to produce a beam with a wavelength of 248 nm. Thereafter, the beam was supplied to a laser micromachining centre (M8000; Exitech, Ltd), where it was passed through a stainless steel mask to produce a  $201 \times 203 \mu\text{m}^2$  rectangular image. The masked beam was then demagnified through a 4x optic (Francis Goodhall, Ltd) to produce an ablation spot with a depth of focus (DoF) of  $6 \mu\text{m}$ . A profile of the masked beam was obtained using a beam profiler (SP620U; Spiricon, Ltd), which showed that the beam shape had an even distribution, with only a slight positive skew across the y-axis; demonstrating good positioning of the mask in the raw beam.

A sample included six machined sites, each produced using 50 pulses in the same machine run with uninterrupted filtered water flow over the sample during machining. The system attenuator was used to change pulse energy by a repeatable amount between sites. Attenuator positions used were: 0.5, 0.6, 0.7, 0.8, 0.9 and 1.0; Figure 2 shows the corresponding fluence values measured using this mask, for ablation in ambient air and under filtered water immersion respectively, that produced features of  $203 \times 205 \mu\text{m}^2$ . This fluence data was calculated from pulse energy data taken using a pulse energy head (J50LP-2, Moletron Detector, Inc.) positioned above the focal point of the laser, and enumerated by a laser energy meter (EM400, Moletron Detector, Inc.). The fluence was calculated using the mean beam energy measured (averaging techniques were employed for experimental rigour: beam pulse energy was recorded five times before and after machining each sample, every value recorded was the mean value measured over 100 pulses - between readings the attenuator was reset to

account for attenuator position errors) so that any changes in laser output over time were accounted for.

### Ambient Air Laser Processing

Samples machined in ambient air were produced, using the same laser and micromachining equipment as the closed flowing thick film filtered water immersion ablation samples. The bisphenol A polycarbonate samples were mounted directly to the vacuum chuck inside the micromachining station (M8000, Exitech, Ltd). After lasing ended the sample was removed and placed into the cell of a sealed sample tray to protect them from atmospheric dust.

### Closed Thick Film Filtered Water Immersion Laser Processing Procedure

Figure 3(a) describes the critical experimental layout of the sample once clamped inside the flow rig, which was mounted to the side of the sample vacuum chuck of the laser micro-processing centre (M8000; Exitech, Ltd.). The sample was positioned in the centre of the flat aluminium table between the water supply and exit holes. The sample was retained by a recess in a spacer plate (to provide a 1.5 mm thick water film) that lay in contact with the aluminium sample table. An O-ring cord, located by a rectangular groove in the sample table, provided a seal between the sample table and the spacer plate. On the top of the spacer plate a second oval O-ring groove was machined to located another O-ring cord. This acted as a gasket between the spacer plate and the beam window – a 25 x 25 x 5 mm<sup>3</sup> ultra-violet grade fused silica sheet (Comar Instruments, Ltd). The beam window was retained by a diamond shaped recess in a third aluminium plate, 8 mm in thickness to provide stiffness to the whole sandwich.

Figure 3(b) shows the water filtering and supply system. Water originated from normal mains supply by wall tap. The water was poured into a domestic water filter (Britta, Inc.) situated at the top the water supply assembly to remove typical corrosive elements present in mains

water. The water was then retained in a header tank located above the pump and, under the action of gravity, was forced into the 700 W pump chamber (CPE100P, Clarke Power Products, Ltd.). The pump forced the water through a water flow rate meter (FR4500, Key Instruments, Inc.) and then along a 3 m distance through a 6 mm outer diameter nylon tube to the inlet push-in elbow fitting on the bottom of the sample table. Last, the water was returned along a further 3 m through a 6 mm outer diameter nylon tube to a collection bucket. The pump was capable of producing 4.2 bar at the outlet, equating to a maximum flow velocity through the ablation chamber of 3.89 m/s, given losses along the supply and return tubing. Precise control of the flow velocity was provided by a variable valve of the flow-meter. Flow velocities of 0.03, 0.11, 1.39, 1.85, 2.31, 2.78, 3.24 and 3.70 m/s were used for this work; the flow rates used to achieve these flow velocity values are given in Table 1.

### Sample Analysis Techniques

The ablation depths were measured using a dragged needle profiler (CM300 Talysurf; Taylor-Hobson, Ltd). Five passes were made across the surface of the sample and into each feature at 50 $\mu$ m intervals. To minimize the possibility of profile error, the mean average depth of each sample feature was then calculated from a selection of three profiles for each sample feature. To guard against outlier samples being produced and effect the ablation threshold measurements taken, all data plotted for interpretation in these results are mean average values taken from the data produced by three sample features machined using each flow velocity.

#### Impact of closed thick film filtered water immersion on ablation threshold.

Ablation threshold is a useful tool for measuring the effectiveness of a technique at etching a material: low threshold fluence indicates that minimal laser energy is required to remove material from a substrate. Figure 4 shows two plots describing the feature depth machined

against the natural log of the laser fluence required. In the standard way, each plot has been fitted with a linear trend line that has been extended to predict the natural log of the minimum laser fluence required to etch the material. The solid trend line in Figure 4 is the etching trend for 248 nm laser radiation in ambient air of bisphenol A polycarbonate; The dashed linear trend line in Figure 4 is an average of the ablation etching trend of 248 nm laser radiation of bisphenol A polycarbonate that has been immersed in a closed filtered water layer (1.5 mm thick) flowing at a number of velocities from 1.39 m/s to 3.70 m/s. This demonstrates that turbulent flow velocity closed thick film filtered water immersion ablation has an average threshold fluence taken from all turbulent flow velocity samples) of  $116.6 \text{ mJ/cm}^2$ , compared the higher value required in ambient air of  $126.1 \text{ mJ/cm}^2$ . Turbulent flow velocity thick film closed filtered water immersion is 7.5% more efficient at etching bisphenol A polycarbonate than laser ablation in ambient air. This is a result that agrees with the previous work of others [22-27], who collectively determined that the increased etching efficiency with respect to laser fluence is due to the action of plume etching. Plume etching occurs when the ablation plume is prevented from expanding by a viscous surrounding medium [22]. Under compression, the gaseous species, initially generated by photonic interaction with the sample, have increased temperature when compared to similar gases inside an ablation plume, it is therefore able to expand with ease. These gasses aggressively attack the surface of the sample, so, restricted plume expansion by use of a viscous surrounding media gives rise to plume etching. This is in contrast to the effects of laser ablation machining under open thin film immersion [11], where the loss in ablation efficiency was accredited to the action a plume motivated rupture. Here, the high pressures initially generated inside the plume, that was initially restricted in growth by the surrounding thin film of de ionized water, rapidly become too high for the thin film of water to contain; resulting in explosive escape of gases from the immersing film. This scenario results in loss of plume etching action, but the

existence of the plume during the laser pulse decreased the magnitude of laser energy arriving at the substrate by the action of *Bremsstrahlung* attenuation; thus both etch mechanisms available are limited by use of an open immersion technique [12].

#### Impact of turbulent flow thick film filtered water immersion on ablation threshold

In Figure 5(a) the etch depth achieved using 248 nm excimer laser ablation on bisphenol A polycarbonate under closed thick film filtered water at six flow velocities ranging from 1.39 m/s to 3.7 m/s in increments of 0.46 m/s, is plotted with respect to the natural logarithm of laser fluence. This allows for the ablation threshold fluence at each flow velocity to be calculated. Table 1 lists the calculated ablation threshold fluences which are plotted in Figure 5(b). All of these samples were produced in a turbulent flow velocity regime ( $Q > 0.88$  m/s), where the filter water flowing over the bisphenol A polycarbonate sample was travelling at sufficient velocity to have a Reynolds number above 4000; thus having a turbulent flow. As can be seen in the plots shown in Figure 5(a), the gradient and x-intercept of all the samples are similar, as confirmed numerically by the trend line gradients offered in the top left of Figure 5(a). This repetition of etch efficiency confirms that the experimental procedure is robust and the closed flowing thick film filtered water immersion technique provided a repeatable and stable medium that ablation can occur within. Despite the apparent similarity of all these plots, the resulting threshold fluence values demonstrate a flow velocity dependent trend that may be explained by interaction between the flowing filtered water and the ablation plume. The plot given in Figure 5(b) shows the threshold fluence of the six samples plotted with respect to the flow in which they were machined. This indicates that achieving minimum threshold fluence requires an optimum flow velocity. Turbulent flows beneath this do not significantly distort the ablation plume, as given in Figure 6(b), causing maximum compression of the plume and maximum traverse distance for the beam through the plume resulting in increased *Bremsstrahlung* attenuation. The optimum flow velocity for

bisphenol A polycarbonate according to the results plotted in Figure 5(b) lies at 3.00 M/s, where the situation drawn in Figure 6(c) occurs, where the flow causes distortion of the plume to reduce traverse distance for the beam through the plume and therefore minimized *Bremsstrahlung* attenuation whilst allowing the existence and action of plume etching by the still compressed ablation plume. Above the optimum flow velocity, the plume is blown away before it can become fully developed, as is the case in figure 6(d), reducing or negating the plume etching effect, leaving only the laser beam, that now has minimal obstacles for possible attenuation to pass through, to etch the material. The small changes to threshold fluence made across this broad range of flow velocities (which corresponds to an increase in flow velocity of 166% from the lowest value plotted in the turbulent flow velocity regime) means that the laser ablation threshold is not critically sensitive to the use of a non-optimum flow velocity.

#### Impact of laminar flow closed thick film filtered water immersion on ablation threshold.

Figure 7 plots the etch depth of the mean average of all the turbulent flow velocity regime samples with respect to the natural logarithm of the fluence along with plots for two samples machined using laminar flow velocity regime closed filter water immersed ablation that both had flow velocities low enough to ensure laminar flow are also given. Threshold fluence values for the laminar flow velocity regime samples are given in Table 1. As has been stated above, the ablation threshold value of the average turbulent flow velocity regime samples has been calculated to be  $116.6 \text{ mJ/cm}^2$ . The sample produced at the highest laminar flow velocity had a threshold fluence of  $125.7 \text{ mJ/cm}^2$ , a value similar to that of the lowest velocity turbulent closed thick film filtered water immersion flow velocity sample, which had an ablation threshold measured at  $126.52 \text{ mJ/cm}^2$ . This result supports the proposal that laminar flow velocities allow the ablation plume to become fully developed inside the liquid

volume, as shown in Figure 6(b), producing maximum *Bremsstrahlung* attenuation of the laser beam. Losses in laser etching due to *Bremsstrahlung* attenuation are then partially compensated for by the action of plume etching being unaffected by the action of the turbulent flow velocity. The samples produced using the slowest flow velocity of all those listed in this work show a very poor correlation. This poor correlation appears to support the idea described schematically in Figure 6(a), where the flow velocity did not have a magnitude sufficient to remove debris produced by one pulse from above the feature before the arrival of the next pulse, resulting in an unreliable laser fluence at the feature.

#### Flow – plume interaction states.

A more detailed explanation of the impact of increasing flow velocity on the ablation threshold under closed thick film flowing filtered water immersion is made clear by Figure 6. The premise of the closed flowing thick film filtered water immersion technique is to entirely clear the image area of debris produced by a laser pulse before the following pulse arrives, thus the velocity of the flow with respect to the pulse frequency is critical. Whereas very low flow velocities do not remove debris reliably between pulses, resulting in unreliable laser fluence at the sample surface (see Figure 6(a)); using a flow velocity that is sufficiently high to fully and reliably clear debris from above the feature, but lower than the optimum flow velocity, causes total etch rate loss due to the *Bremsstrahlung* attenuation of the fully developed compressed ablation plume, (see Figure 6(b)). But, this loss is compensated for by the etching action of the plume (see Figure 6(b)). The optimum flow velocity is achieved when the immersing liquid washes a proportion of the ablation plume away during the laser pulse, not allowing excessive *Bremsstrahlung* attenuation, but simultaneously not completely destroying the ablation plume, thereby preserving the action of plume etching, a state illustrated by Figure 6(c). When greater than optimum flow velocities are used they allow maximum laser etching, the high viscosity of a liquid medium will deform the ablation plume

during the laser pulse, reducing the plume etching mechanism described in the literature [24-27] by removing the ablation plume before it has fully developed (see Figure 6(d)). These four states are described in terms of etching contribution by laser and plume by the hypothetical plot in Figure 8. The data generated in this work shows that direct laser ablation etching is still the dominant factor in this interaction, as the curve in Figure 5(b) describes. When the plume becomes fully developed, *Bremsstrahlung* attenuation has a far greater limiting effect on the ablation threshold than high flow velocities washing away the compressed ablation plume. The optimal flow velocity for achieving minimal threshold fluence is achieved by a compromise, indicated by the dashed vertical line in Figure 8, where the combination of laser etching and compressed plume etching result in an increased etch rate greater than the maximum etch rate achievable by either of the component etch mechanisms alone. This plot shows the dependence of plume etching on the existence of significant laser etching, as laser etching is required to develop an ablation plume that can then go on to become compressed and begin etching itself. The plume etch rate declines as the immersing liquid flow velocity begins to wash the ablation plume away at higher velocities, leaving just the action of laser etching, at mechanism that relies on mechanical and chemical interactions [19, 20].

The average ablation threshold fluence can be plotted with respect to the closed thick film filtered water immersion fluid flow velocity (see Figure 9). Initial inspection of Figure 8 supports the states described in detail above. Sub optimum turbulent flow produced a maximum threshold, measured to be  $126.52 \text{ mJ/cm}^2$ , denoting poor etching efficiency, where high *Bremsstrahlung* attenuation limited laser etching, the size of the plume and therefore the aggressive etching action of the compressed hot gasses inside a water immersed plume, as described to the left of Figure 8. As the flow velocity is increased towards the optimum threshold value of  $111.76 \text{ mJ/cm}^2$ , the ablation threshold fluence drops. This is what one

would expect to happen as the magnitude of laser etching and plume etching increased together. As the flow velocity rises beyond 3.24 m/s to the maximum magnitude tested, the threshold fluence begins to rise slightly again to 115.71 mJ/cm<sup>2</sup>, where the ablation plume was beginning to be washed away before it was able to become fully developed, leaving only the action of laser etching to remove material.

#### Importance of fluence on ablation threshold under closed thick film filtered water immersion.

The previous discussions only take into account the average ablation threshold measured across all laser fluences. If the data is split to high fluence data and low fluence data, two plots can be generated; these show a clear contrast to each other. In Figure 10(a) high laser pulse fluence data is plotted. This data shows the turbulent flow velocity regime samples had significantly lower threshold fluences than high fluence ambient air samples. The threshold fluence increased drastically to a value of 399.16 mJ/cm<sup>2</sup> for the lowest flow velocity. In contrast, the low laser pulse fluence data, plotted in Figure 10(b), had significantly reduced threshold fluence for the very low flow velocity and greatly increased threshold fluences for the turbulent flow velocity regime data. The two filter water plots appear to be mirror images of each other about the threshold fluence of bisphenol A polycarbonate in ambient air. This can be explained by returning to the theory of confined ablation plumes [22] and the drag imparted onto it by the liquid flowing over it. At laminar flow velocities the plume generated was not removed, it was able to become fully developed and etch the sample as it lay under compression. High fluence resulted in significant *Bremsstrahlung* attenuation, hence a high threshold fluence. Low fluence laser pulses always perform well for etch efficacy in ambient air because they do not produce large plumes and waste energy with heating *via* multi photon interactions [14] a fact demonstrated by the magnitude of the threshold fluence in ambient air in Figure 10(b). Any etching provided by the plume to supplement this efficient removal by

low fluence pulses significantly increased the etch rate with respect to the laser energy supplied, causing the low threshold fluence recorded for the lowest flow velocity. As the flow velocity increased to the turbulent flow velocity regime, the ablation plume was removed, allowing maximum laser etching without any *Bremsstrahlung* attenuation that limits high fluence pulse efficiency in air. This was of no aide to power pulses, that lost the supplementary action of plume etching with the deletion of the ablation plume, removing any advantage over ablation in ambient air. Losses due to attenuation of the equipment, such as the flow chamber window, which was 5 mm thick and the immersing filtered water itself, resulted in the increased recorded threshold fluence for turbulent flow velocity closed filtered water immersion ablation evident in Figure 10(b).

### Conclusions

The use of turbulent flow velocity regime closed thick film filtered water immersion ablation results in an average decrease in ablation threshold of 7.5%, compared to ablation using a similar beam in ambient air. This is the result of the combined action of laser etching and ablation plume etching, which is a symptom of the plume pressure being increased as the expansion of the plume is restricted by viscous surrounding liquid medium.

Conversely, laminar flow velocity regime closed thick film filtered water immersion ablation results in a decrease in ablation threshold of just 0.3% compared to ablation using a similar beam in ambient air; thus, it can be likened to a negligible gain. This is interesting as it suggests a shift in ablation mechanism.

To investigate this theory, the effect of flow velocity on the ablation threshold has been recorded. All plots of the feature depth machined into bisphenol A polycarbonate using 50 pulses of KrF excimer laser radiation under turbulent flow velocity closed thick film filtered water immersed ablation with respect to the natural log of the laser fluence display similar gradients. Plotting the threshold fluence values projected from this data against the flow

velocity they were produced with results in a plot trend of subtle but interesting significance: to achieve minimum threshold fluence, an optimum flow velocity exists: measured in this work to be 3.00 m/s. This effect is credited to a flow velocity dependent shift in ablation mechanism relating to the distortion of the ablation plume by the flowing volume of immersion liquid. At lower flow velocities the ablation plume remained directly above the feature during the entirety of the pulse, thus generating maximum *Bremsstrahlung* attenuation and limiting laser etching (and as a result plume etching). As the flow velocity climbed, an optimum condition was found where the ablation plume geometry was distorted by the flowing immersion fluid in a manner that simultaneously allowed lower *Bremsstrahlung* attenuation and maximum plume etching, that combine to produce increased etch efficiency than the laser beam alone. With further increase of the flow velocity the ablation plume was completely destroyed by the flowing immersion fluid, negating *Bremsstrahlung* attenuation and allowing unimpeded laser etching coupled with negligible plume etching.

Laminar flow velocity immersion was limited by another factor: suspended debris beam attenuation. The flow was slow enough to cause debris produced by one pulse to remain suspended over the site of the feature as the following pulse arrived; therefore, intercepting the beam *en route* to the feature. This gave rise to the scenario of non linear etch rate over 'n' pulses.

The effect of closed thick film filtered water immersion on ablation threshold has been shown to vary with respect to beam fluence. For high fluence beams, the ablation threshold was significantly reduced when compared to ablation in ambient air at turbulent flow velocities. Conversely, for low fluence beams all but the lowest flow velocity tested showed significant increase in ablation threshold over a similar beam in ambient air. This is attributed to the action of plume etching being flow velocity dependant. For high fluence beams, the removal of the plume allows maximum laser etching, but when using low fluence beams, the

significant relative attenuation posed by the closed flowing thick film filtered water immersion equipment became a serious disadvantage when compared to ablation in ambient air.

## References

1. Rizvi, N. H., Apte, P. “Developments in laser micro-machining techniques”, Journal of Materials Processing Technology, 2002, **127**, pp.206-210
2. Dyer, P. E. “ Excimer laser polymer ablation: twenty years on”, Applied Physics A, 2003, **77**, pp.167-173
3. Gower, M. C. “Excimer laser microfabrication and micromachining”, Laser Precision Microfabrication, RIKEN Review, 2001, pp.50-56.
4. Braun, A., Zimmer, K., Hösselbarth, B., Meinhardt, J., Bigl, F., Mehnert, R. “Excimer laser micromachining and replication of 3D optical surfaces”, Applied Surface Science, 1998, **127-129**, pp.911-914
5. Izatt, J. A., Sankey, N. D., Partovi, F., Fitzmaurice, M., Rava, R. P., Itzkan, I., and Feld, M. S. “Ablation of Calcified Biological Tissue Using Pulsed Hydrogen Fluoride Laser Radiation”, IEEE Journal of Quantum Electronics, 1990, **26**, 12, pp.2261-2270.
6. Ghantasala, M. K., Hayes, J. P., Harvey, E. C., and Sood, D. K. “Patterning, electroplating and removal of SU-8 moulds by excimer laser micromachining”, Journal of Micromechanics and Microengineering, 2001, **11**, pp.133-139.
7. Lankard J. R., and Wolbold, G., “Excimer Laser Ablation of Polyimide in a Manufacturing Facility”, Applied Physics A, 1992, **54**, pp.355-359
8. Lobo, L. M., “Solid Phase By-Products of Laser Material Processing”, Doctoral Thesis, 2002, Loughborough University
9. Dowding, C. F. and Lawrence, J. “Use of thin laminar liquid flows above ablation area for control of ejected material during excimer machining”, The proceedings of The 27th International Congress on Application of Lasers and Electro-Optics: Laser Materials Processing Section, 2008, pp.872-880.

10. Dowding, C. F., and Lawrence, J. "Use of thin laminar liquid flows above ablation area for control of ejected material during excimer machining", IMECHE Proceedings B, 2009, **223**, 6, pp.
11. Dowding, C. F., and Lawrence, J. Analysis of the excimer laser ablation characteristics of bisphenol A polycarbonate in ambient air and under thin film laminar flow water immersion. The proceedings of The 27th International Congress on Application of Lasers and Electro-Optics: Laser Materials Processing Section, 2008, pp.202-211.
12. Dowding, C. F., and Lawrence, J. "Impact of open de-ionized water thin film laminar immersion on the liquid immersed ablation threshold and ablation rate of features machined by KrF excimer laser ablation of bisphenol A polycarbonate", Optics and Lasers in Engineering, Accepted for Publication, 2009.
13. Phipps, C. R. "Laser Ablation and its Applications" 2007, Springer. NL.
14. Crafer, R., and Oakley, P. J. Laser Processing in Manufacturing, 1993, Chapman & Hall, London.
15. Xu, X. F., "Phase explosion and its time lag in nanosecond laser ablation", Applied Surface Science, 2002, **197**, pp.61-66.
16. Xu, X. F., and Song, K. H. "Phase change phenomena during high power laser-materials interaction", Materials Science and Engineering: A - Structural Materials Properties Microstructure And Processing, 2000, **292**, 2, pp.162-168.
17. Kelly, R., and Miotello, A. "On the role of thermal processes in sputtering and composition changes due to ions or laser pulses", Nuclear Instruments & Methods In Physics Research Section B: Beam Interactions With Materials And Atoms, 1998, **141**, 1-4, pp.49-60.

18. Lee, S. K., Chang, W. S., and Na S. J. “Numerical and experimental study on the thermal damage of thin Cr films induced by excimer laser irradiation”, *Journal of Applied Physics*, 1999, **86**, 8, pp.4282-4289.
19. Pataulf, G., and Dyer, P. “Photomechanical Processes and Effects in Ablation”, *Chemical Review*, 2003, **103**, 2, pp.487-518.
20. Georgiou, S., and Koubenakis, A. “Laser-Induced Material Ejection from Model Molecular Solids and Liquids: Mechanisms, Implications, and Applications”, *Chemical Review*, 2003, **103**, 2, pp.349–394.
21. Prasad, M., Conforti, P. F., and Garrison, B. J. “Coupled molecular dynamics-Monte Carlo model to study the role of chemical processes during laser ablation of polymeric materials”, *Journal of Chemical Physics*, 2007, **127**, 8.
22. Berthe, L., Fabbro, R., Peyre, P., and Toller, L. “Shock waves from a water-confined laser-generated plasma”, *Journal of Applied Physics*, 1997, **82**, 6, pp.2826-2832
23. Zhu, S., Lu, Y. F., Hong, M. H., Chen, X. Y., “Laser ablation of solid substrates in water and ambient air”, *Journal of Applied Physics*, 2001, **89**, 3, pp.2400-2403
24. Fabbro, R., Peyre, P., Berthe, L., and Scherpereel, X. L. “Physics and applications of laser-shock processing“, *Journal of Laser Applications*, 1998, **10**, 6, pp.265-269.
25. Elaboudi, I., Lazare, S., Belin, C., Talaga, D., and Labrugere C. “Underwater excimer laser ablation of polymers”, *Applied Physics A*, 2008, **92**, 4, pp.743-748.
26. Elaboudi, I., Lazare, S., Belin, C., Talaga, D., and Labrugere C. “From polymer films to organic nanoparticles suspensions by means of excimer laser ablation in water”, *Applied Physics A*, 2008, **93**, 4, pp.827-831.
27. Elaboudi, I., Lazare, S., Belin, C., Talaga, D., and Labrugere C. “Organic nanoparticles suspensions preparation by underwater excimer laser ablation of polycarbonate”, *Applied Surface Science*, 2007, **253**, 13, pp.7835-7839.

28. Richerzhagen, B “Material shaping device with a laser beam which is injected into a stream of liquid”, Synova S.A., 1999, **WO/1999/056907**, Switzerland.
29. Dyer, P. E., Key, P. H., Sands, D., Snelling, H. V., and Wagner, F. X. “Blast-wave studies of excimer laser ablation of ZnS”, Applied Surface Science, 1995, **86**, pp.18-23.
30. Wang. J., Niino. H., Yabe. A. “Micromachining of transparent materials with superheated liquid generated by multiphotonic absorption of organic molecule” Applied Surface Science, 2000, **154–155**, pp.571–576.
31. Kopitkovasa. G., Lipperta. T., David. C., Wokauna. A., and Gobrechtb. J. “Fabrication of micro-optical elements in quartz by laser induced backside wet etching”, Microelectronic Engineering, 2003, **67–68**, pp.438–444.
32. Kopitkovasa. G., Lipperta. T., David. C., Wokauna. A., and Gobrechtb. J. “Surface micromachining of UV transparent materials”, Thin Solid Films, 2004, **453–454**, pp.31–35.

### List of Tables

Table 1: List of ablation threshold fluences at varying flow velocities. Values plotted in Figure 4(b).

### List of Figures

Figure 1(a): open flow – causes an uneven drag profile, generating rolling turbulence in the manor described by the black vectors. Generation of turbulence always occurs after a characteristic flow displacement, dependant upon fluid properties. Figure 1(b): closed flow – symmetrical drag profile, generating a flow velocity profile similar to that described by the grey arrows. The generation of turbulence is dependent upon flow velocity; laminar flow-rates do not generate turbulent flow.

Figure 2: A comparison of beam fluence generated at various attenuator positions recorded for both the filtered water samples and the ambient air samples

Figure 3(a): the closed immersion ablation assembly: 1) sample; 2) base plate; 3) sample clamp and flow chamber spacer; 4) U.V. grade fused silica window for laser beam; 5) window clamp; 6) clamping bolts that squeeze components together. Figure 3(b): the fluid supply unit: 1) source water; 2) filtering; 3) filtered water storage; 4) centrifugal pump; 5) flow-rate control valve; 6) high pressure flow-rate controlled filtered water outlet to flow-rate ablation chamber.

Figure 4: Two plots describing the etch depth achieved using 50 pulses of varying laser beam fluence in ambient air and the average etch depth achieved using 50 pulses of varying laser beam fluence across all turbulent flow velocities tested under closed thick film filtered water

Figure 5(a): a detailed set of plots describing the ablation threshold of six different samples machined under turbulent velocity regime closed thick film filtered water immersion. Figure 5(b): a plot of the etch depth dependency on flow velocity of bisphenol A polycarbonate immersed by filtered water.

Figure 6(a): when the flow-rate is laminar and the laser pulse frequency is high, the liquid flow may not remove all of the debris before the next pulse arrives, thus the suspended debris may obscure the pulse, effecting the machined profile; Figure 6(b): a flow velocity lying below the optimum allows the ablation plume to fully develop, maximizing *Bremsstrahlung* attenuation and near compensating by uninhibited plume etching; Figure 6(c): the optimum condition occurs when the flowing liquid distorts the ablation plume to minimize *Bremsstrahlung* attenuation, without removing the action of plume etching; Figure 6(d) when using a very high flow velocity with respect to the pulse width of the laser the ablation plume may become distorted by the viscosity of the fluid. This may have an impact on plume etch rate.

Figure 7: a graph comparing the average ablation threshold achieved using turbulent flow velocity regime thick film closed immersion ablation and two laminar flow velocity regime thick film closed immersion machined samples.

Figure 8: a schematic plot showing the action and combination of plume etching and laser etching and the flow velocity dependence of both. An optimum point exists and is depicted by the dashed vertical line, where the summation of both etching mechanisms combines to maximum effect.

Figure 9: a comparison of average threshold fluence measured at all thick film closed immersion flow velocities against the ablation threshold in ambient air.

Figure 10(a): a comparison of the average threshold fluence measured for high fluence pulses at all thick film closed immersion flow velocities against the ablation threshold in ambient air. Figure 10(b): a comparison of the average threshold fluence measured for low fluence pulses at all thick film closed immersion flow velocities against the ablation threshold in ambient air.

Table 1

Flow Rate (l/min)	Flow Rate (l/s)	Flow Velocity (m/s)	Threshold Fluence (mJ/cm <sup>2</sup> )
2.00	0.033	3.70	115.7
1.75	0.029	3.24	111.8
1.50	0.025	2.78	114.1
1.25	0.021	2.31	113.0
1.00	0.017	1.85	118.6
0.75	0.013	1.39	126.5
0.06	0.001	0.11	125.7
0.015	0.00025	0.03	See text

Figure 1

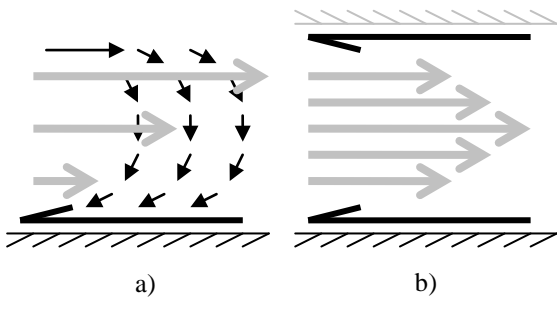


Figure 2

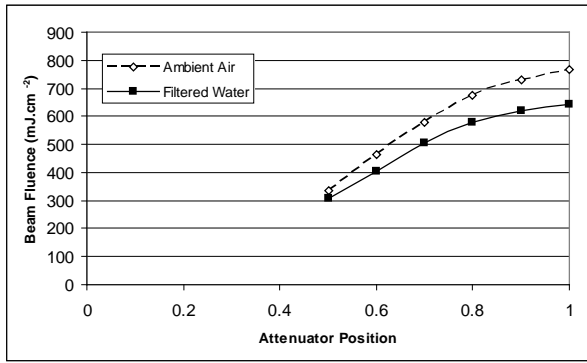


Figure 3

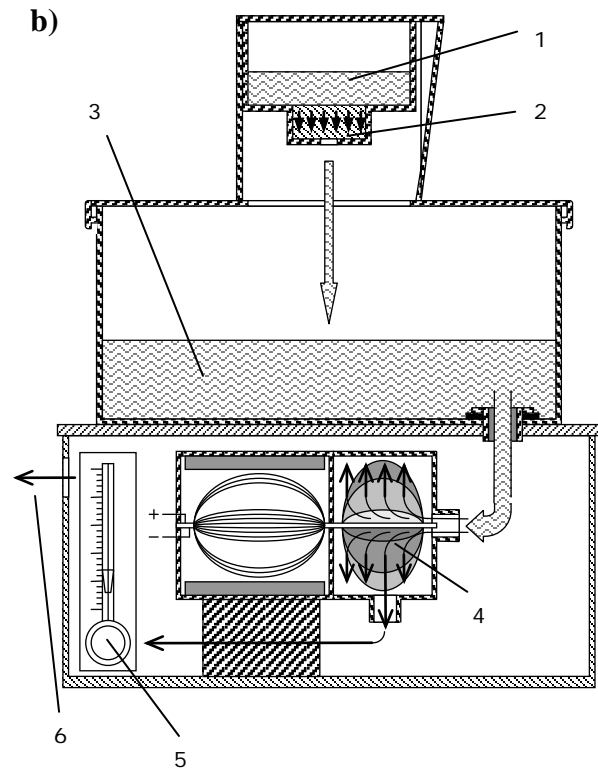
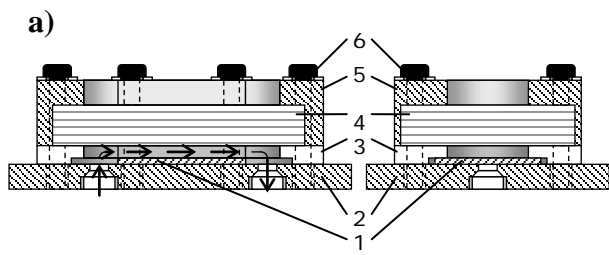


Figure 4

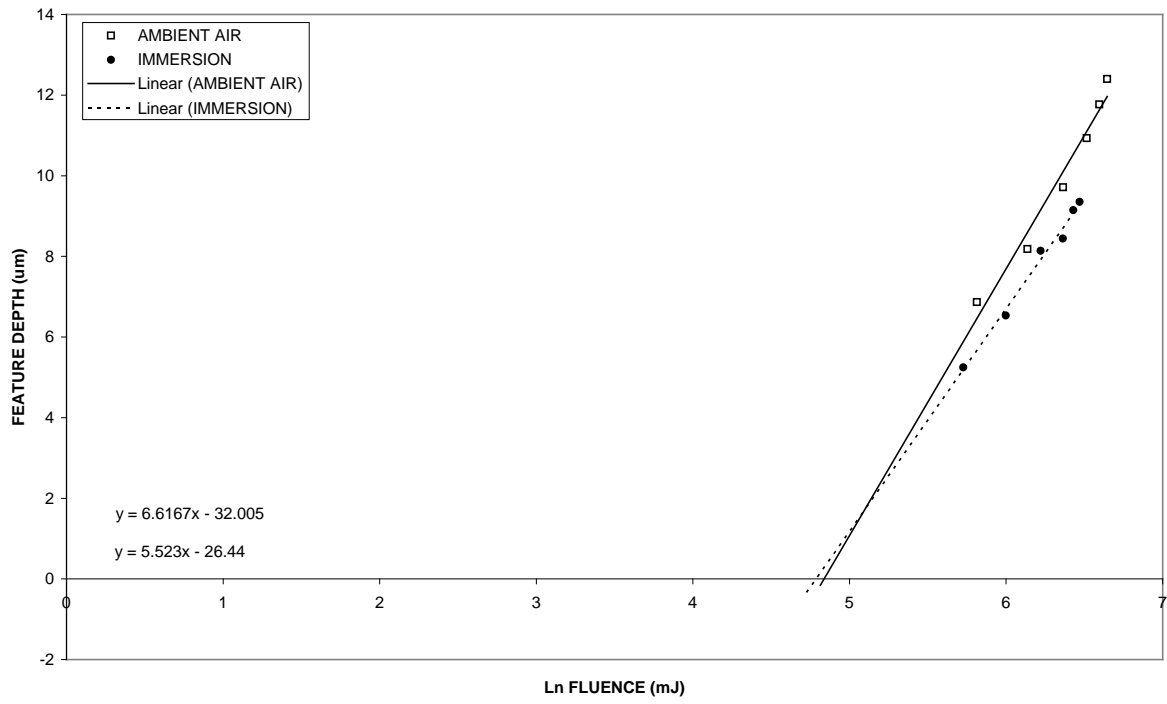


Figure 5(a)

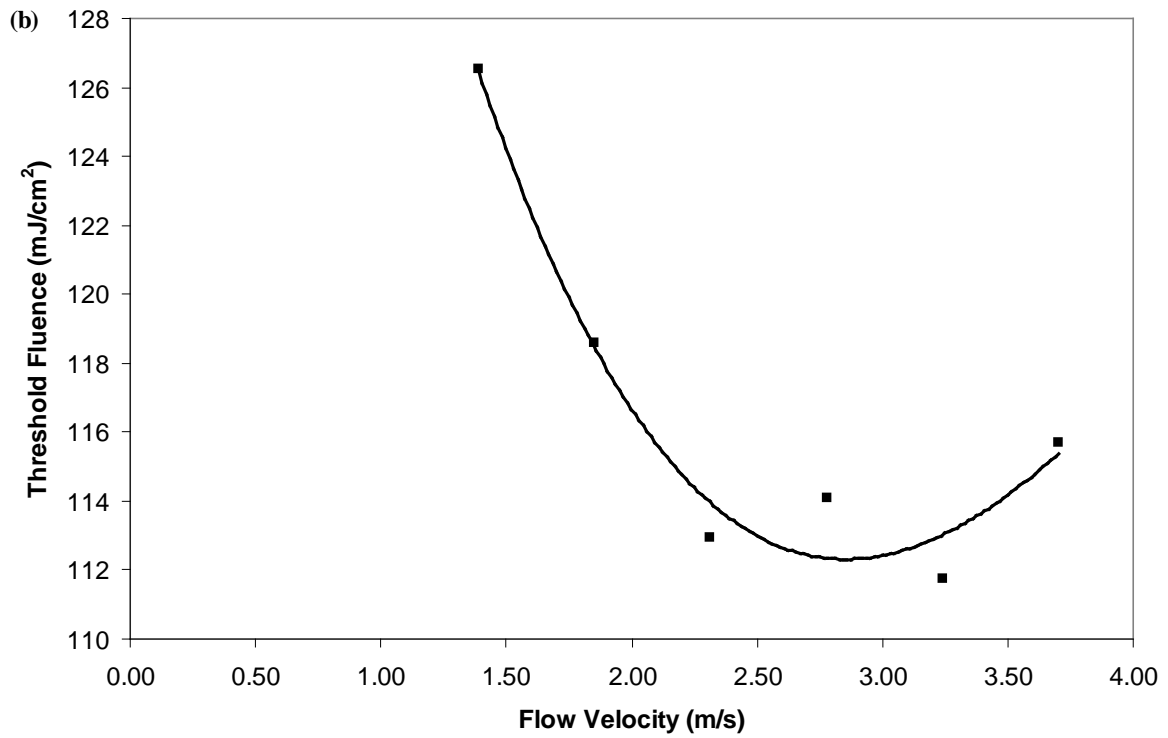
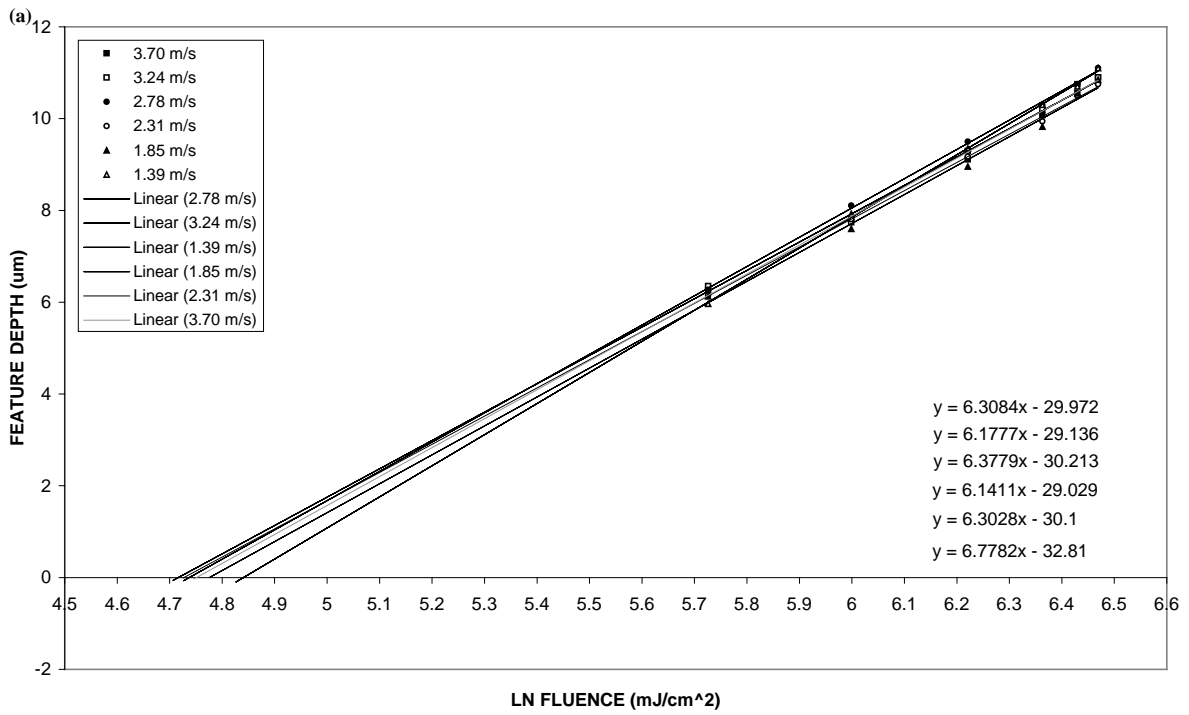


Figure 6

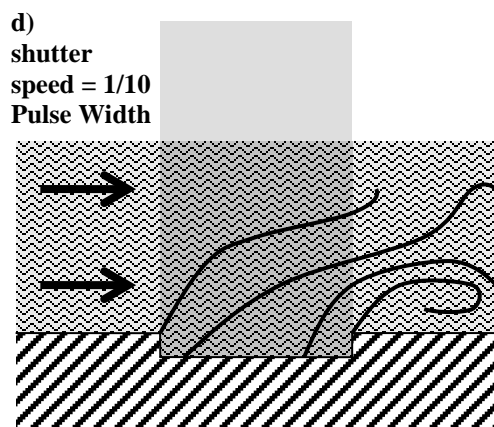
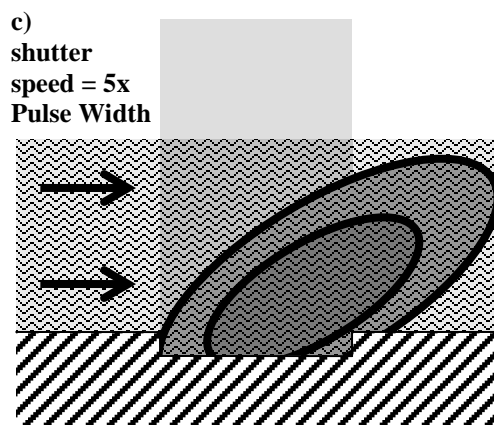
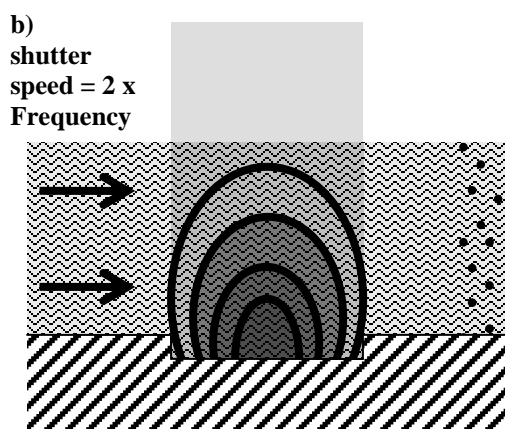
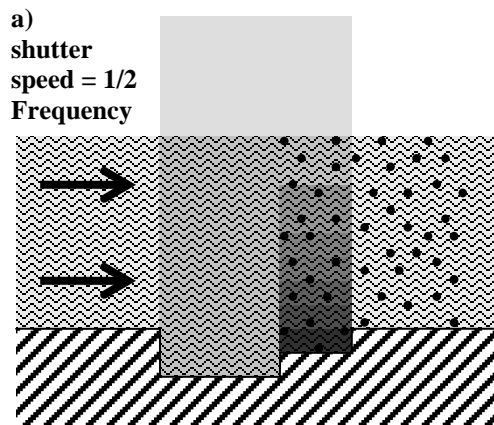


Figure 7

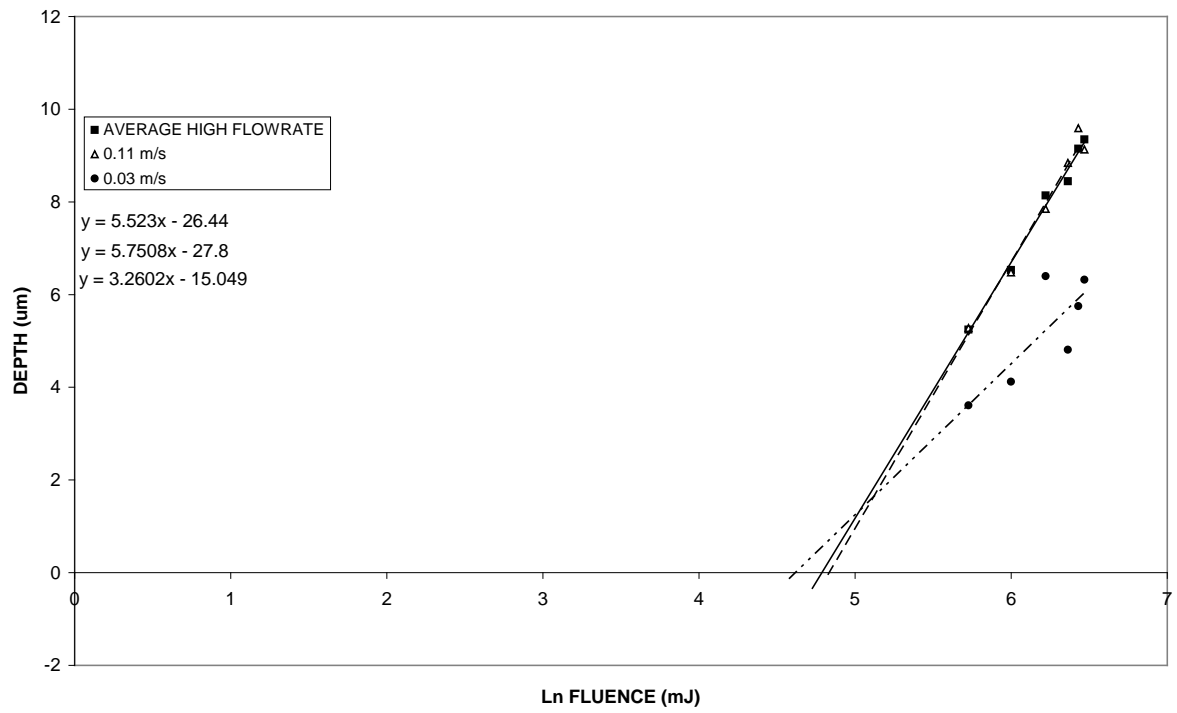


Figure 8

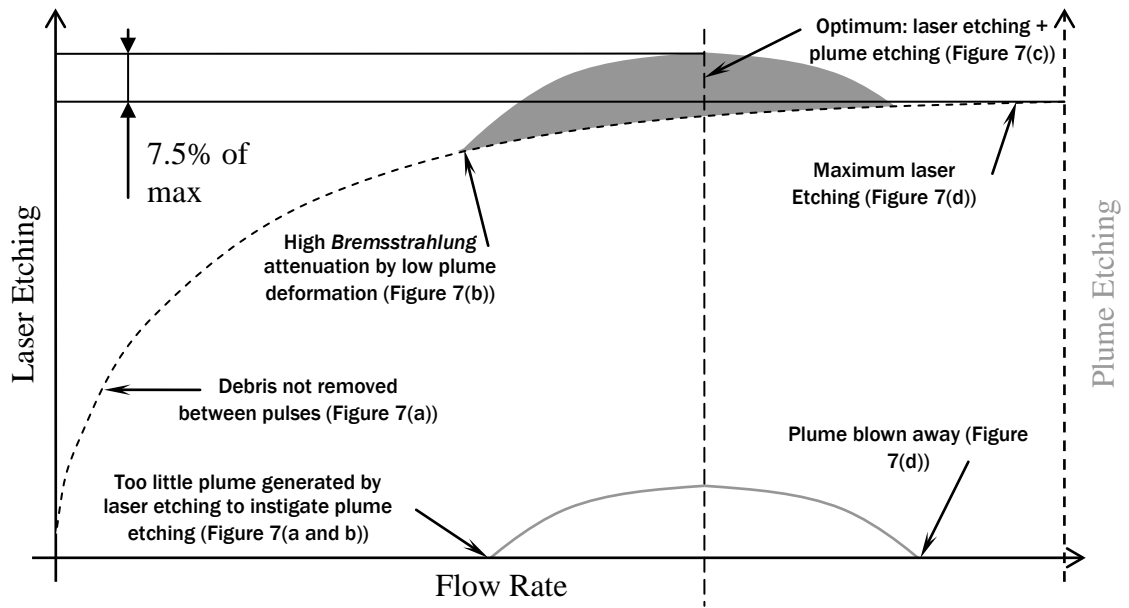


Figure 9

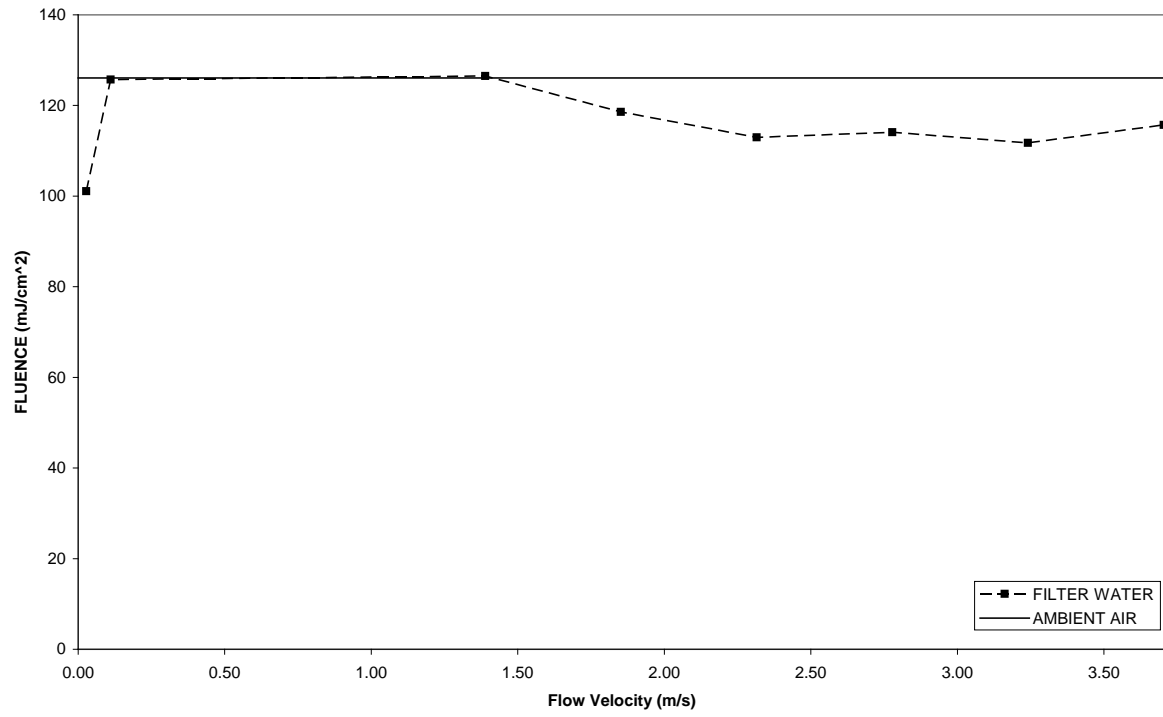


Figure 10

